A&A 466, 831–838 (2007)
DOI: 10.1051/0004-6361:20066235

Astronomy & Astrophysics

The ISOPHOT 170 μm Serendipity Survey

III. FIR statistics of optically identified galaxies⋆

M. Stickel, U. Klaas, and D. Lemke

Max-Planck-Institut für Astronomie, Königstuhl 17, 69117 Heidelberg, Germany
e-mail: stickel@mpia.de

Received 11 August 2006 / Accepted 7 November 2006

ABSTRACT

Aims. To shed more light on the integrated FIR properties of galaxies, the ≈2000 compact sources in the ISOPHOT Serendipity Survey associated with identified galaxies are investigated statistically. They provide the only sample large enough to determine the FIR properties such as dust temperatures and masses, FIR luminosities, and HI-to-dust ratios not only for the group as a whole, but also divided into several subgroups of different Hubble types. Only with this catalog, the high flux end of the 170 μm galaxy number counts can be established, which is crucial as a complement to the much deeper ISOPHOT studies at this wavelength in much smaller sky areas.

Methods. The differential distributions of integrated FIR properties and the cumulative number counts are analysed.

Results. The galaxy list of the ISOPHOT Serendipity Survey has a 170 μm completeness limit of ≈2 Jy. The statistical analysis confirmed that the $F_{170\ \mu m}/F_{100\ \mu m}$ flux ratios peak at ≈1, corresponding to a dust color temperature of ≈20 K. FIR luminosities and dust masses cover a large range with peaks near $L_{1-1000} \approx 10^{10.5\pm1}\ L_{\odot}$ and $M_{\rm Dust} \approx 10^{7.5\pm0.5}\ M_{\odot}$, respectively. HI-to-dust ratios range from ≈10 and ≈10^4, rendering the notion of fiducial HI-to-dust ratio for conversion between gas and dust masses almost useless. The latest models of the cumulative 170 μm number counts are in reasonable agreement with the deep as well as the shallow surveys from ISO up to fluxes of ≈50 Jy.

Key words. surveys – infrared: galaxies – infrared: general – galaxies: ISM

1. Introduction

By including the important wavelength range beyond the IRAS limit of 100 μm, the ISOPHOT instrument (Lemke et al. 1996; Lemke & Klaas 1999) aboard the Infrared Space Observatory (ISO, Kessler et al. 1996; Kessler 1999) has opened a new window for the statistical investigation of the FIR properties of normal galaxies. Several studies of this type have been carried out through pointed observations of restricted samples of optically selected galaxies (e.g., Alton et al. 1998; Siebenmorgen et al. 1999; Contursi et al. 2001; Bendo et al. 2002; Tuffs et al. 2002) designed to investigate different aspects of the galaxy population (see also review by Tuffs & Popescu 2005). The survey of Bendo et al. (2002) was optimized to provide 60 μm, 100 μm, and 170 μm surface brightnesses of the central regions of bright resolved spiral galaxies ($B_{\rm T} < 12$) from the Revised Shapley-Ames Catalogue. The ISOPHOT Virgo Cluster Deep Survey of Tuffs et al. (2002), by virtue of observing a nearby cluster sample, was able to probe the faintest local universe galaxy population reachable with ISOPHOT at 60 μm, 100 μm, and 170 μm. In fact, even today in the Spitzer era, it is still the deepest survey of normal galaxies in the local universe. However, the structural information and deepness afforded by the above-mentioned surveys necessarily precluded the measurement of galaxies in statistically large numbers. With its large number of slews and the achieved significant sky coverage, the ISOPHOT Serendipity Survey (Lemke & Burgdorf 1992; Bogun et al. 1996) represents the largest sky survey at 170 μm to date. The sky coverage and the selected collections of sources are necessarily incomplete (Stickel et al. 2003), but the slew data are nevertheless very useful because they contain the largest unbiased source samples currently available, which have been measured at this wavelength.

The dust grains in galaxies are heated to a wide range of temperatures. Although these systems are far from homogeneous, they can be approximated to the first order as having two major components: A warm dust component, which is tracing dust locally heated by star-forming regions, and a cold dust component, primarily diffusely distributed in the disk (Tuffs & Popescu 2005). The bulk of the dust luminosity in galaxies is carried by dust grains heated to temperatures in the range 10−30 K. Their spectral energy distribution (SED) peaks in the Far-Infrared (FIR) between 100 μm and 200 μm, which hitherto has only been accessible to ISO. Since the derived FIR luminosities and dust masses are very sensitive to the coldest dust component present, the FIR measurements beyond the IRAS 100 μm limit are essential in characterizing the FIR properties of galaxies and provide the only direct way for the correct decomposition and interpretation of FIR and sub-mm data.

Flux measurements up to 100 μm together with sub-mm data can be reconciled with a 15−20 K dust component dominating the FIR SED beyond 100 μm, but also with a much weaker component from even colder dust in conjunction with a much warmer dust component (Chini et al. 1995). Sub-mm data alone can

⋆ Based on observations with ISO, an ESA project with instruments funded by ESA Member States (especially the PI countries: France, Germany, The Netherlands, and the UK) and with the participation of ISAS and NASA. Members of the Consortium on the ISOPHOT Serendipity Survey (CISS) are MPIA Heidelberg, ESA ISO SOC Villafranca, AIP Potsdam, IPAC Pasadena, Imperial College London.

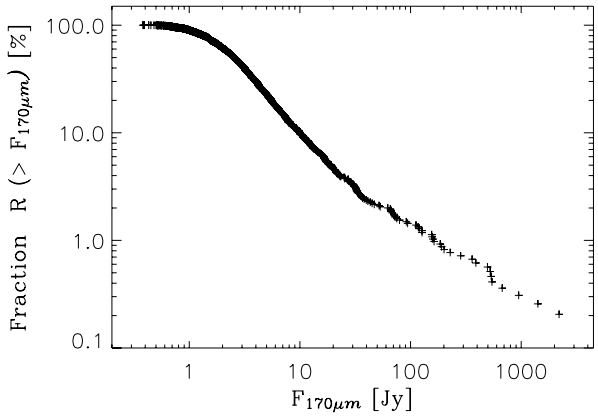

Fig. 1. The cumulative log N – Log S diagram for all optically identified galaxies. The straight part between ≈2 Jy and ≈50 Jy can be represented by a power law with a slope of ≈−1.2, at lower fluxes a significant flattening is noticeable.

never provide the necessary constraints for the derivation of dust color temperatures (Holland et al. 2003). Eventually, dust temperature estimates and derived dust masses based on the IRAS 60 μm and 100 μm fluxes alone are extremely unreliable, as the 60 μm flux can significantly be influenced by transiently heated small particles (Mathis 1990; Popescu et al. 2000). The 170 μm ISOSS measurements are thus bridging the important but largely unexplored wavelength gap from the IRAS 100 μm limit to the sub-mm measurements.

Only the Serendipity Survey contains the necessary flux measurements near the peak of the SED at 170 μm for a very large number of compact sources, which allow more reliable estimations of their FIR properties. The analysis of the compact sources, with special emphasis on galaxies, as well as the resulting compact source database is described in Stickel et al. (1998a,b, 2000, 2004). The compact sources associated with galaxies, in particular, provide a sample large enough to investigate the distributions of their FIR properties such as dust temperatures and masses, FIR luminosities, and HI-to-dust ratios not only as a whole, but also divided into several subgroups of different Hubble types. Based on the catalog of 170 μm measurements for all compact ISOPHOT Serendipity Survey sources associated with known optically identified galaxies (Stickel et al. 2004), a detailed statistical analysis of the FIR properties of these galaxies is given. This investigation vastly extends the initial FIR statistics of galaxies from the ISOPHOT Serendipity Survey presented in Stickel et al. (2000).

2. Completeness of the galaxy catalog

The full cumulative Log N−Log S diagram (Fig. 1) for all galaxies including the nearby resolved objects (Stickel et al. 2004) can be approximated by two power laws, a flatter one for the flux range above ≈50 Jy, and a steeper one with a slope of ≈−1.2 for the flux range 2−50 Jy. A total of 1167 sources have fluxes above 2 Jy, while only 26 sources are above 50 Jy. Below ≈2 Jy, the slope of the counts shows a significant flattening. Assuming that the counts are actually continuously rising, this flattening indicates that the completeness limit of the catalog has been reached at ≈2 Jy, and not all fainter galaxies have been selected from the source candidate database. This result is in agreement with the completeness statistics based on IRAS sources described in the investigation of the North Ecliptic Pole Minisurvey (Stickel et al. 1998a), where the detection rate also decreased sharply below 2 Jy.

Table 1. Basic sample statistics for sources in the catalog of optically identified Serendipity Survey galaxies.

total number of sources	1927
sources with fluxes ...	
... >0.5 Jy	1920
... >1.0 Jy	1726
... >2.0 Jy	1167
... >5.0 Jy	423
... >10.0 Jy	175
sources with tabulated redshifts	1628
sources with $F_{170\ \mu m}/F_{100\ \mu m}$ ratios	1733
sources with FIR luminosities	1499
sources with FIR luminosities and morphologies ...	1499
...of optical type "E/S0"	112
...of optical type "S"	498
...of optical type "SA"	103
...of optical type "SAB"	129
...of optical type "SB"	214
...of optical type "I "	89
...of optical type "Other"	78
...of optical type "No"	276
sources with dust masses and morphologies ...	1501
...of optical type "E/S0"	113
...of optical type "S"	498
...of optical type "SA"	102
...of optical type "SAB"	131
...of optical type "SB"	214
...of optical type "I"	90
...of optical type "Other"	77
...of optical type "No"	276
sources with dust masses and HI data ...	677
...of optical type "E/S0"	46
...of optical type "S"	206
...of optical type "SA"	54
...of optical type "SAB"	63
...of optical type "SB"	78
...of optical type "I"	37
...of optical type "Other"	32
...of optical type "No"	161

3. Statistics of far-infrared properties

The auxiliary data such as 100 μm and 60 μm fluxes, redshifts, optical morphologies, and HI masses necessary to derive physical quantities are incomplete to a highly varying degree, which results in a strongly varying number of sources for which various quantities such as dust luminosities and dust masses can be computed. Table 1 collects the basic source statistics.

3.1. Color temperatures

The distribution of the $F_{170\ \mu m}/F_{100\ \mu m}$ flux ratios for 1733 galaxies with an IRAS counterpart within 3′ (Fig. 2) shows a peak near $F_{170\ \mu m}/F_{100\ \mu m} \approx 1$, indicating that most galaxies have a rather flat FIR SED between 100 μm and 200 μm. There is a sharper drop towards lower flux ratios, implying that an SED decreasing from 100 μm to 170 μm is seen only in relatively few galaxies having a dominating warm dust component. A long tail extends out to higher $F_{170\ \mu m}/F_{100\ \mu m}$ flux ratios, which is due to an up-turn in the SED beyond 100 μm similar to that seen in the Milky Way and M 51 (Chini & Krügel 1993). Overall, the distribution is quite similar to that of the initial list of well observed

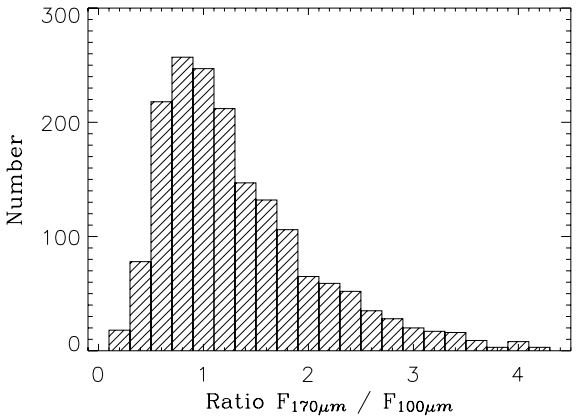

Fig. 2. The distribution of the ratio of Serendipity Survey 170 μm and IRAS 100 μm fluxes for all optically identified galaxies, which have an IRAS source closer than 3′. Most of the galaxies have a 170 μm/100 μm flux ratio of ≈1.

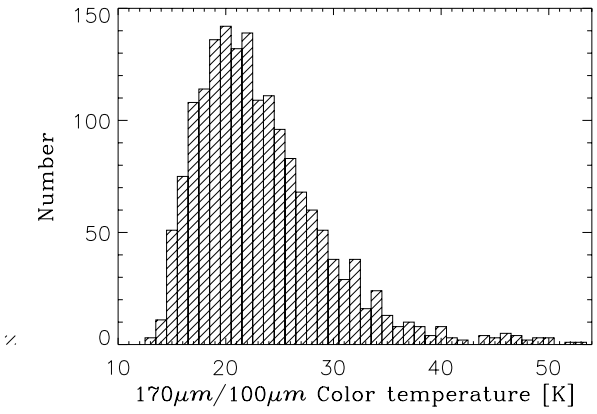

Fig. 3. The color temperature distribution, corrected for the ISOPHOT 170 μm and IRAS 100 μm bandpasses derived using an emissivity index of $\beta = 2$. The broad distribution has its peak at $T_{\rm Dust} \approx 20$ K, with a range between 13 K and 40 K.

galaxies (Stickel et al. 2004), but, with 20 times the number of objects, is now much better statistically verified.

The distribution of the $F_{170\,\mu\rm m}/F_{100\,\mu\rm m}$ flux ratios clearly indicates the presence of a cold dust component ($F_{170\,\mu\rm m}/F_{100\,\mu\rm m} \gtrsim 2$) in a significant fraction of the galaxies. Since the color corrections for the IRAS as well as the ISOPHOT broad-band fluxes refer to a spectrum with νF_ν = constant, dust color temperatures were computed by iteratively correcting the tabulated IRAS 100 μm and Serendipity 170 μm fluxes in the two bandpasses for a modified blackbody (Planck) function

$$F_\nu \propto \nu^\beta \, B_\nu \, (T_{\rm Dust}), \tag{1}$$

with a fixed emissivity index $\beta = 2$. Varying the assumed emissivity index between 2 and 0 for $F_{170\,\mu\rm m}/F_{100\,\mu\rm m}$ flux ratios of 1, 2, and 3 increases the derived dust temperatures by 18 K, 8 K, and 5 K, respectively.

Color temperatures derived from Eq. (1) are upper limits to the cold dust temperatures as the IRAS 100 μm fluxes contain contributions from warmer dust heated by star-forming regions. The distribution (Fig. 3) has its peak at $T_{\rm Dust} \approx 20$ K, with all but a few sources lying in the range $13\,{\rm K} \lesssim T_{\rm Dust} \lesssim 40\,{\rm K}$. This is again in good agreement with the more sparse distribution of dust color temperatures from the smaller sample of centrally crossed Serendipity Survey galaxies (Stickel et al. 2004).

Remarkably, the median color temperature of the lower luminosity Virgo Cluster sample is ≈15 K, significantly lower than that of the ISOSS galaxy sample (≈20 K, Fig. 3). Since the latter samples have higher galaxy luminosities in general, there appears to be a trend of increasing dust color temperature with optical and/or FIR luminosities. Such a trend has already been noted by Popescu et al. (2002) and Tuffs & Popescu (2005), based on the much smaller group of centrally crossed Serendipity Survey galaxies (Stickel et al. 2004), which is now confirmed with a much larger sample.

The presence of very cold dust with temperatures well below 15 K can in principle be established with ISOPHOT data alone, namely by finding objects with a steeply increasing FIR SED between 100 μm and 200 μm. While such SEDs have been measured in cold galactic sources, galaxies with such a cold dust component apparently are rare, at least in the current collection of the ISOSS galaxies. The distribution of dust color temperatures (Fig. 3) show only very few objects below 15 K. In the ISOPHOT Virgo Cluster Deep Survey (Tuffs et al. 2002), several of the optically fainter galaxies have FIR SEDs that can only be reconciled with a very cold dust component with temperatures down to ≈10 K (Popescu et al. 2002). The relatively high optical and FIR flux limit of the ISOSS galaxy sample might preferentially contain objects with a quite significant star formation rate, which is heating the dust, so that a sample going to fainter FIR fluxes might have a better chance to detect a larger fraction of very cold galaxies.

3.2. FIR luminosities

With the addition of a third flux measurement at 170 μm to the two IRAS 60 μm and 100 μm wavelengths, the integrated FIR flux F_{40-220} in the wavelength range between 40 μm and 220 μm can be written as

$$F_{40-220} = 1.34 \times 10^{-14} \times (2.58\, F_{60\,\mu\rm m} + 1.00\, F_{100\,\mu\rm m} + 0.63\, F_{170\,\mu\rm m})\ [{\rm W\,m^{-2}}], \tag{2}$$

where the relation is valid within ≈±20% for dust temperatures between 20 K and 80 K and emissivity indices $0 \le \beta \le 2$. This formula is similar to the one given by Helou et al. (1988) for the IRAS 60 μm and 100 μm fluxes and extends the coverage to 220 μm assuming a square-wave bandpass, which is 180 μm wide and centered at 132.5 μm.

For the temperature range between 20 K and 80 K, the ratio of F_{40-220} and the total integrated IR flux F_{1-1000} in the wavelength range between 1 μm and 1000 μm depends rather sensitively on the assumed temperatures and emissivity indices. This reflects the strong dependence of the shape of a modified blackbody on temperature and emissivity indices, when the region beyond its peak is covered by the broad ISOPHOT C_160 filter centered at 170 μm. However, for the coldest dust components with temperatures of 15−30 K, which comprises the vast majority of the sources in Fig. 3, the ratio F_{1-1000}/F_{40-220} varies much less and the total integrated IR flux can be written as

$$F_{1-1000} = 1.35\, F_{40-220}\ [{\rm W\,m^{-2}}], \tag{3}$$

which is accurate to within ≈±30% for emissivity indices $0 \le \beta \le 2$.

From the integrated IR fluxes, total IR luminosities L_{1-1000} can be derived by

$$L_{1-1000} = 4\,\pi\, D^2\, F_{1-1000}, \tag{4}$$

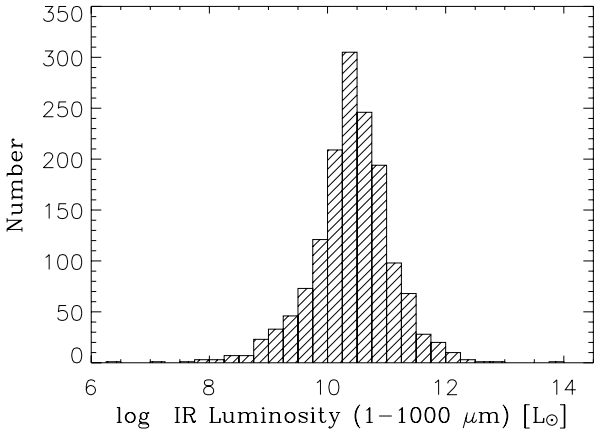

Fig. 4. The distribution of total FIR luminosities, derived from the ISOPHOT 170 μm and the IRAS 60 μm and 100 μm fluxes. Sources with $L_{1-1000} \gtrsim 10^{12}\,L_\odot$ are classified as ultraluminous. The source with the lowest luminosity is NGC 205.

where D is the luminosity distance. Galaxy distances were computed from the redshifts ($H_0 = 75\,\mathrm{km\,s^{-1}\,Mpc^{-1}}$, $q_0 = 0.5$) for all but the nearby sources with $cz < 1000\,\mathrm{km\,s^{-1}}$, which in turn were taken from the literature. The distribution of L_{1-1000} luminosities for 1499 galaxies with an IRAS source nearer than 3′ and available redshifts (Fig. 4) shows a broad peak at $L_{1-1000} \approx 10^{10.5\pm1}\,L_\odot$, covering the large range from galaxies with low FIR luminosities to starburst and luminous infrared galaxies. For comparison, the IR luminosity of the Milky Way is about $\approx 1.2 \times 10^{10}\,L_\odot$ (Telesco 1988), while starburst galaxies like M 82 and NGC 253 have IR luminosities in the range $(3-6) \times 10^{10}\,L_\odot$ (Sanders & Mirabel 1996).

The distribution of L_{1-1000} luminosities separated according to the morphological type is shown in Fig. 5. The E/S0 and Irr types a significantly broader distribution with tails extending to low luminosities, while all spiral types are remarkably similar. A marked shift towards high luminosities is apparent for other morphological types and those galaxies without classification. The latter group is necessarily biased since it contains the highest redshift objects in the sample, which can only be detected if the luminosities are higher than average.

There is one source with a very low FIR luminosity of $\approx 10^{6.5}\,L_\odot$, well separated from the other sources, which is the spheroidal galaxy NGC 205 (M 110), a companion of M 31. Sixteen sources lie above the threshold to ultraluminous infrared galaxies ($L_{1-1000} \gtrsim 10^{12}\,L_\odot$), and only three have $L_{1-1000} \gtrsim 10^{12.5}\,L_\odot$, namely the QSO ISOSS J 18218+6421 (KUV 18217+6419) and the galaxies ISOSS J 13179−1548 (IRAS 13153−1532) ISOSS J 15307+6309 (IRAS 15298+6319). The high FIR luminosity of the former source can be ascribed to its nature as a QSO, where the IR luminosity is powered either by a strong starburst and/or by the central active galactic nucleus (e.g., Haas et al. 2003). The latter two sources, however, appear as rather inconspicuous and resolved galaxies on optical DSS images. Since the redshift of ISOSS J 13179−1548 (IRAS 13153−1532) has already been questioned on the basis of its optical appearance, its apparently extremely high FIR luminosity might therefore be highly overestimated. In a similar vein, the redshift of ISOSS J 15307+6309 (IRAS 15298+6319) might equally well be too high. Both sources should be reobserved to shed more light on their nature, particularly to investigate whether they might belong to the rare class of gravitational lenses similar to the ultraluminous IRAS source F 10214+7425 (Broadhurst & Lehar 1995).

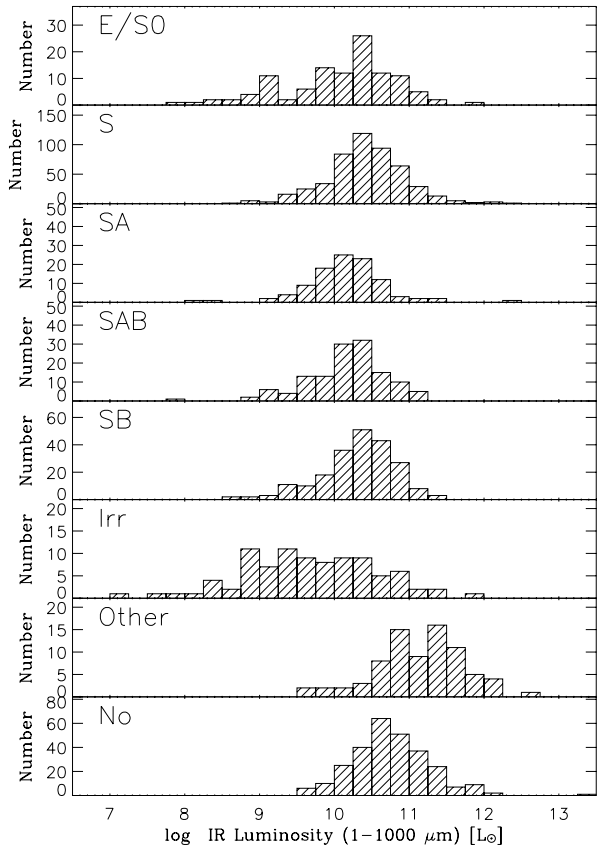

Fig. 5. The distribution of total FIR luminosities separately for the various Hubble types.

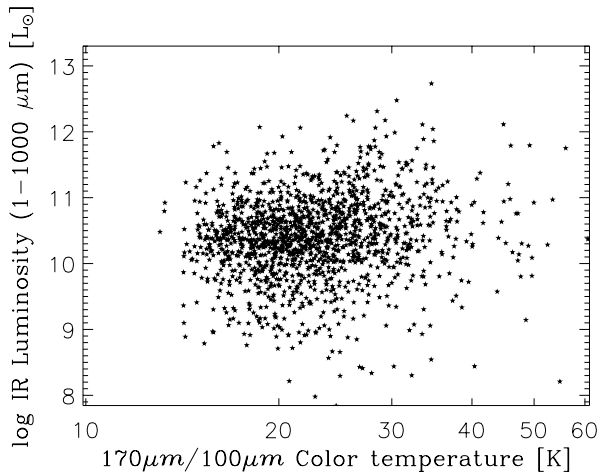

Fig. 6. The distribution of total FIR luminosities vs. the dust temperatures. A weak trend of increasing dust temperature with increasing FIR luminosity seems to be present.

3.3. Dust masses

To model far infrared SEDs and calculate dust masses it would be desirable to use properly calculated models derived from radiative transfer codes and detailed grain models. Such models have been applied to small samples (Silva et al. 1998; Popescu et al. 2000; Misiriotis et al. 2001). Since the cold dust dominates

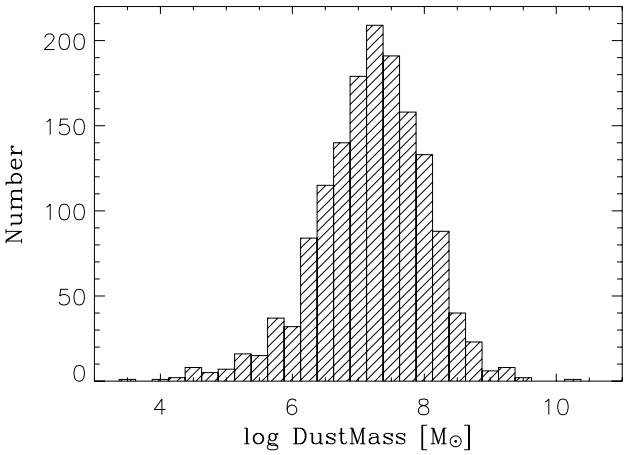

Fig. 7. The distribution of dust masses, derived using the 170 μm fluxes, the dust color temperatures, an emissivity index of $\beta = 2$, and a dust opacity value of 3 m^2/kg. The distribution is somewhat asymmetric and peaks near $M_{\rm Dust} \approx 10^{7.5\pm1}\ M_\odot$.

the total dust mass, a safe lower limit to the dust mass can be obtained by assuming that all dust grains in the galaxies are at the dust color temperature derived above (Fig. 3). The mass of the emitting dust $M_{\rm Dust}$ can then be estimated from

$$M_{\rm Dust} = D^2\ F_\nu\ [\kappa_\lambda\ B_\nu\,(T_{\rm Dust})]^{-1} \quad (5)$$

(Hildebrand 1983; Draine 1990), where F_ν is the flux density, D the distance, κ_λ the dust opacity, and $T_{\rm Dust}$ the dust color temperature. Dust opacities are rather uncertain and for 170 μm a representative value of 3 m^2/kg was used, which lies in the middle of the range given by Draine (1990).

The dust masses as derived from the 170 μm fluxes and the dust temperatures for 1501 galaxies (Fig. 3) via Eq. (5) show a somewhat asymmetric distribution (Fig. 7), quite similar to the much smaller sample shown in Stickel et al. (2004). The peak again lies near $M_{\rm Dust} \approx 10^{7.5\pm0.5}\ M_\odot$, with a somewhat broader tail towards smaller dust masses. This value is about an order of magnitude larger than the median value of the dust masses obtained for the Virgo Cluster and Bright Galaxies Sample of Popescu et al. (2002) and Bendo et al. (2002), respectively. This might indicate that the Serendipity Survey by virtue of its relatively high flux limit samples the more FIR luminous galaxy populations.

The distribution of dust masses separated according to the Hubble types of the optical counterparts is shown in Fig. 8, where uncertain classifications have been added to the corresponding classes. The panel labeled "other" contains all those galaxies where the classification is not of the ususal Hubble types, but mostly an activity indicator such as "HII" or "Sy", while "No" contains all galaxies without any optical morphological information. There appears to be no significant differences between the spiral galaxies of various types, i.e., barred and unbarred spirals are quite similar in their dust content. However, the dust masses of spheroidal (E/S0) and irregular galaxies do reach significantly lower values. Other types and unclassified types appear to have systematically higher dust masses, which might be due to the inclusion of sources at systematically higher redshifts, which in turn does not allow a clear optical morphological categorization from the available optical direct imaging data.

Recent deep blind surveys in the sub-mm have revealed a large population of sources hardly detectable at any other wavelength (e.g., Blain et al. 2002). The currently favored interpretation is that these sources are high-redshift equivalents of the local

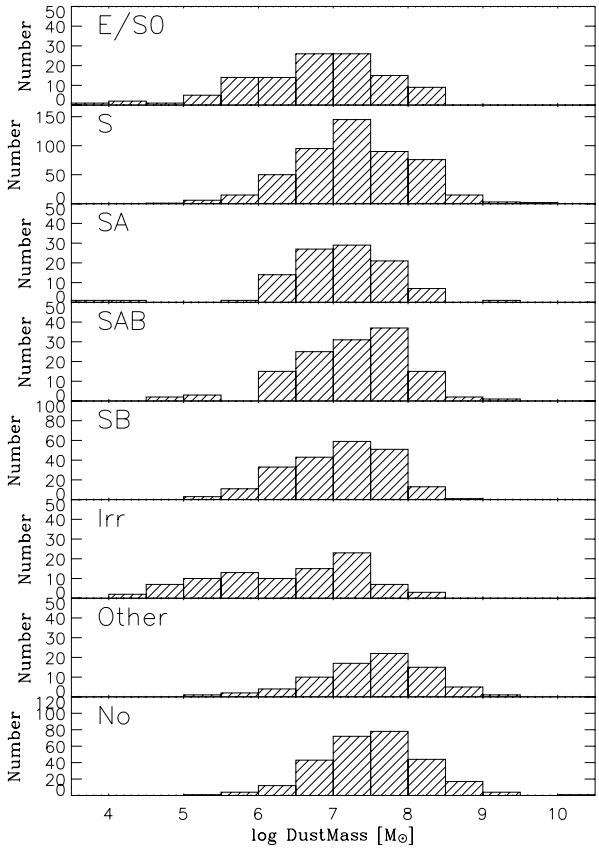

Fig. 8. The distribution of dust masses for the various Hubble types separately. Uncertain classifications have been included in the corresponding class. A tendency for on average lower dust masses is apparent for the spheroidal (E/S0) and irregular (Irr) galaxy types. Galaxies with other or even no morphological classification tend to have the highest dust masses, indicating that higher redshifts accompany insufficient optical morphological data.

ultraluminous galaxies discovered by IRAS, having FIR SEDs dominated by warm dust with temperatures above 40 K. An alternative explanation for the sub-mm sources would be massive galaxies with a very large amount of cold dust with temperatures in the range 15−25 K, similar to what is found in the current sample of normal local galaxies. Total FIR luminosities of $\gtrsim 10^{12}\ L_\odot$, typical of ultraluminous galaxies, would then require total dust masses of $\approx 10^9\ M_\odot$, depending strongly on the dust temperature. Since most of the galaxies have dust masses of $\approx 10^{7.5}\ M_\odot$ (Fig. 3), this would be a mass increase of roughly a factor of 50. Because of the lower dust temperatures, the photometric redshifts derived from the FIR and sub-mm SEDs would then be much smaller than the now favored range of $2 \lesssim z \lesssim 5$. As a result of the Malmquist bias, such objects should show up in flux limited samples like the Serendipity Survey just above the detection limit with redshifts higher than the majority of sources. Indeed, one such local source is the above mentioned ultraluminous cold elliptical ISOSS J 15049+7247 ($z \approx 0.2$), where the combined IRAS-ISOPHOT data together with 1.3 mm follow-up measurements give a dust temperature of ≈21 K, a dust mass of $\approx 5 \times 10^8\ M_\odot$, and a total FIR luminosity of $\approx 2 \times 10^{12}\ L_\odot$ (Krause et al. 2003).

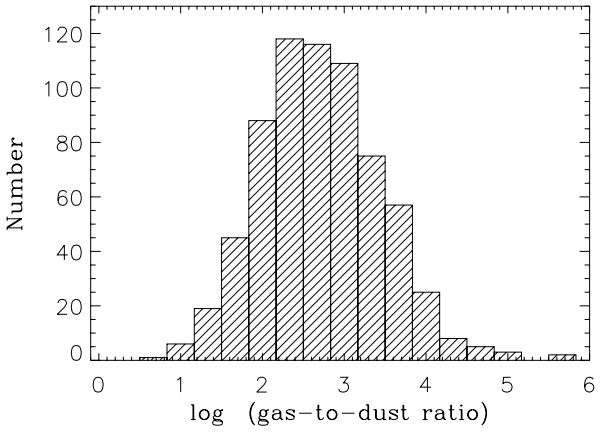

Fig. 9. The distribution of HI-to-dust mass ratios is rather broad, covering a large range of values between 10 and 10^4.

3.4. HI-to-dust ratios

Gas masses from HI measurements were collected for those galaxies with an IRAS source within 3′ and available redshift by querying the LEDA database (Paturel et al. 1995), which uncovered measurements for roughly one third (677 sources) of the complete list. The HI-to-dust ratio distribution (Fig. 9) shows a broad peak with a median value of ≈500, which is somewhat higher than the canonical value of the Milky Way (≈160, Sodroski et al. 1994). Again, the derived HI-to-dust ratios cover the large range between ≈10 and $\approx 10^4$, as found for the smaller initial galaxy sample (Stickel et al. 2004). From IRAS data alone, a range between ≈500 and ≈2000 had been found, with an average of ≈1000 (Devereux & Young 1990). A similar large range for the HI-to-dust ratio has been found by Popescu et al. (2002), although their median value of about 100 was significantly smaller. Bendo et al. (2002) used CO measurements to derive gas-to-dust ratios refering to the molecular component only, but again found a large range.

Although the average of the HI-to-dust ratio with dust masses from the 170 μm Serendipity Survey fluxes is close to the galactic value, the spread is nevertheless larger than expected from uncertainties in the FIR fluxes or gas masses. This can be taken as evidence that the spread of the HI-to-dust ratio reflects a property of the galaxies in the sample and that there is no fiducial, well defined HI-to-dust ratio applicable to all normal late-type galaxies to convert HI masses to dust masses or vice versa. This might be due to the different galaxy morphologies, or could possibly be also an age effect from the continuous transformation of gas into dust via the stellar evolution, or a result from gas or dust removal during gravitational interactions, or be related to the overall metallicity of the galaxies.

This is supported by the distribution of the HI-to-dust ratio separated according to morphological types (Fig. 10). Galaxies of all categories show a rather broad distribution covering the whole range of HI-to-dust ratios seen in the full distribution (Fig. 9). The early types E/S0 might even have an indication of a bimodal distribution. This might be due to the fact that this category is comprised of two sub-groups, where the ellipticals (E) have little gas and dust remaining from their evolutionary track, as it is commonly assumed, and S0 galaxies, which could have acquired their larger amount of gas by external processes such as interactions. It should be mentioned that the separation of E from S0 galaxies is not always easily possible and subject to substantial discrepancies in the literature, which makes the interpretation of their gas-to-dust distribution difficult.

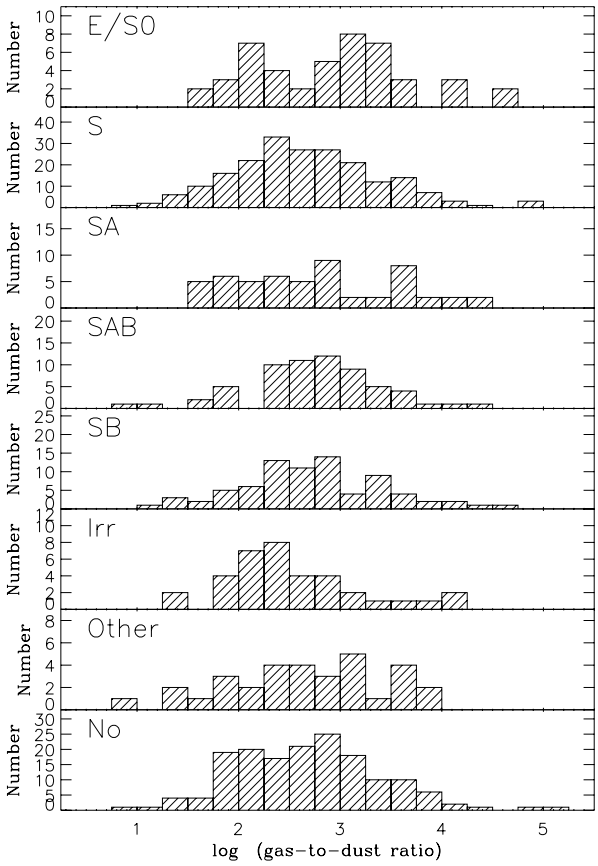

Fig. 10. The distribution of HI-to-dust mass ratios, separately for the different Hubble types.

4. FIR number counts

Several surveys with ISOPHOT at wavelengths beyond 100 μm have attempted to derive cumulative FIR number counts (Juvela et al. 2000; Dole et al. 2001; Kawara et al. 2004) and tried to compare the results with theoretical model predictions. It was found that no-evolution models cannot account for the observed source counts. Rather, an evolving luminous infrared galaxy population was required. Restricted by observing time limitations, only relatively small areas were covered, so that only sources with $F_{170\,\mu\mathrm{m}} \lesssim 1$ Jy could be counted in statistically significant numbers. Additional source densities were estimated from IRAS 100 μm data using a mean $F_{170\,\mu\mathrm{m}}/F_{100\,\mu\mathrm{m}}$ flux ratio (Puget et al. 1999; Linden-Vørnle et al. 2000). The models of Guiderdoni et al. (1998), Franceschini et al. (2001), Rowan-Robinson (2001), and Takeuchi et al. (2001) predict number counts at 170 μm down to ≈10 μJy, while the predictions at the bright end start at ≈10 Jy. More recently, Lagache et al. (2004) used improved galaxy SEDs and evolutionary parameters to predict number counts for a wide variety of wavelengths and over a large flux range up to ≈100 Jy.

Only the Serendipity Survey with its large sky coverage is able to provide constraints and actual source densities for the bright end of the 170 μm number counts. The integral counts from the full galaxy catalog for all sources with $F_{170\,\mu\mathrm{m}} > 2$ Jy including the resolved galaxies (Fig. 11) shows a power law slope of ≈ -1.2 in the flux range $2\,\mathrm{Jy} < F_{170\,\mu\mathrm{m}} < 20\,\mathrm{Jy}$, significantly flatter than the steep density increase towards fainter flux levels (Juvela et al. 2000; Dole et al. 2001; Kawara et al. 2004). A further flattening appears to be present for $F_{170\,\mu\mathrm{m}} > 20$ Jy, but this could be due to the inclusion of galaxy density

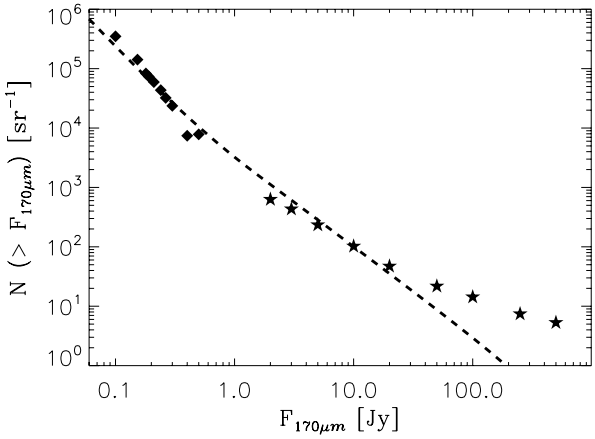

Fig. 11. The 170 μm number counts from the Serendipity Survey Galaxy Catalog ($F_{170\ \mu m} \gtrsim 2$ Jy; asterisks) and deeper ($F_{170\ \mu m} \lesssim 1$ Jy; diamonds) small-area ISOPHOT surveys (Dole et al. 2001; Kawara et al. 2004; Juvela et al. 2000) reveal a continuous steepening towards lower fluxes. The dashed line represents the latest model from Lagache et al. (2004).

enhancements and superstructures (Local Supercluster, the Centaurus cluster, etc.) of the local universe in the Serendipity Survey area. The only models with a significant flattening at the bright end are that of Rowan-Robinson (2001) and Lagache et al. (2004), the latter of which comes closest to the actual observed source density (Fig. 11).

Almost all model predictions agree that the source density at $F_{170\ \mu m} = 1$ Jy is approximately one per square degree, corresponding to $\approx$3300 sr^{-1}, which is quite close to the extrapolation of a power law in the range 2 Jy $< F_{170\ \mu m} <$ 20 Jy to 1 Jy. Most models simply have a Euclidian slope of -1.5 at the bright end. The extrapolation of such a density law to, e.g., 100 Jy would underpredict the actual source density by at least a factor of five, but for the reasons given above this is not a strong argument against the validity of current models and the overall agreement between observations and models is quite good.

All compact sources from the Serendipity Survey entering Fig. 11 are identified with known galaxies, while all deeper surveys have just assumed that all detected sources are indeed associated with galaxies. This, however, has been somewhat hard to prove observationally (Scott et al. 2000; Sajina et al. 2003) and the possibility still exists that an unknown fraction of the FIR sources from the deeper small-scale 170 μm surveys are actually galactic cirrus structures. This would require a downward correction of the deep counts and would obviously bring them closer to the extrapolation from the faint end of the Serendipity Survey galaxy counts near 2 Jy. The far-reaching consequences, namely that a fraction of $\approx$10% of the cosmological background light has already been resolved at these FIR wavelengths (Juvela et al. 2000; Dole et al. 2001), might thus have been somewhat premature. In fact, the most recent optical/NIR follow-up observations of sources from the deep ELAIS/FIRBACK surveys of ISO revealed that the vast majority are actually star-forming galaxies of quite modest redshifts (Dennefeld et al. 2005; Taylor et al. 2005).

On the other hand, if there is a non-negligible group of as yet unidentified galaxies among the compact Serendipity Survey sources, they would not have been included in the current galaxy catalog. Such a group would steepen the faint end slope of the number counts, and thereby bring them more in agreement with the deep counts. A cross-correlation with galaxies identified in the 2MASS or SDSS thus appears warranted, to check whether additional galaxies not yet listed in databases such as NED and Simbad can be found among the compact Serendipity Survey sources.

5. Concluding remarks

The concept of a serendipitous and incomplete but unbiased slew survey at FIR wavelengths, implemented into the European ISO mission as the ISOPHOT Serendipity Survey, has proven to be highly successful. It provided the largest catalog of 170 μm flux measurements for a wide variety of different galaxy types, which allowed the study of the FIR properties of galaxies over a wide range of morphological types for the first time.

The 170 μm number counts between $\approx$2 Jy and $\approx$50 Jy are reasonably well determined, and are in agreement with the most recent models. To increase the number of observed galaxies at the highest fluxes above 50 Jy and to eventually fix the bright-end slope of the 170 μm number counts requires an all-sky survey at FIR wavelengths, such as the one carried out with the ongoing Japanese satellite FIR mission AKARI (formerly ASTRO-F). With its vastly increased sample size, this survey also has the prospect of allowing an even more detailed view of the FIR properties as a function of optical morphological galaxy type.

Acknowledgements. We particularly thank Richard Tuffs and Cristina Popescu for generously sharing their extensive and very constructive comments and suggestions on an earlier version of the manuscript with us, which significantly improved its final quality. We further thank the referee, Tsutomu T. Takeuchi, for his useful remarks to strengthen the presentation of our results. The development and operation of ISOPHOT were supported by MPIA and funds from Deutsches Zentrum für Luft- und Raumfahrt (DLR). The ISOPHOT Data Centre at MPIA is supported by Deutsches Zentrum für Luft- und Raumfahrt (DLR) with funds of Bundesministerium für Wirtschaft und Technologie, grant No. 50 QI0201.
This research has made use of NASA's Astrophysics Data System Abstract Service, the Simbad Database, operated at CDS, Strasbourg, France, and data from the Infrared Processing and Analysis Center (IPAC) and the NASA/IPAC Extragalactic Database (NED), which are operated by the Jet Propulsion Laboratory, California Institute of Technology, under contract with the National Aeronautics and Space Administration.

References

Alton, P. B., Trewhella, M., Davies, J. I., et al. 1998, MNRAS, 335, 807
Bendo, G. J., Joseph, R. D., Wells, M., et al. 2002, AJ, 123, 3067
Blain, A. W., Smail, I., Ivison, R. J., Kneib, J.-P., & Frayer, D. T. 2002, Phys. Rep., 369, 111
Bogun, S., Lemke, D., Klaas, U., et al. 1996, A&A, 315, L71
Broadhurst, T., & Lehar, J. 1995, ApJ, 450, L41
Burgdorf, M. 1990, Dissertation, University of Heidelberg, Germany
Chini, R., & Krügel, E. 1993, A&A, 279, 385
Chini, R., Krügel, E., Lemke, R., & Ward-Thompson, D. 1995, A&A, 295, 317
Contursi, A., Boselli, A., Gavazzi, G., et al. 2001, A&A, 365, 11
Dennefeld, M., Lagache, G., Mei, S., et al. 2005, A&A, 440, 5
Devereux, N. A., & Young, J. S. 1990, ApJ, 359, 42
Dole, H., Gispert, R., Lagache, G., et al. 2001, A&A, 372, 364
Draine, B. T. 1990, in The Interstellar Medium in Galaxies, ed. H. A. Thronson Jr., & J. M. Schull (Dordrecht: Kluwer), 483
Franceschini, A., Aussel, H., Cesarsky, C. J., Elbaz, D., & Fadda, D. 2001, A&A, 378, 1
Guiderdoni, B., Hivon, E., Bouchet, F. R., & Maffei, B. 1998, MNRAS, 295, 877
Haas, M., Klaas, U., Müller, S. A. H., et al. 2003, A&A, 402, 87
Helou, G., Khan, I. R., Malek, L., & Boehmer, L. 1988, ApJS, 68, 151
Hildebrand, R. H. 1983, QJRAS, 24, 267
Holland, W. S., Duncan, W. D., Greaves, J. S., et al. 2003, SCOWL: a large format submillimeter camera on the Overwhelmingly Large Telescope. Proc. SPIE, 4840, 340
Juvela, M., Mattila, K., & Lemke, D. 2000, A&A, 360, 813
Kawara, K., Matsuhara, H., Okuda, H., et al. 2004, A&A, 413, 843
Kessler, M. F., Steinz, J. A., Anderegg, M. E., et al. 1996, A&A, 315, L27

Kessler, M. F. 1999, in The Universe as seen by ISO, ed. P. Cox, & M. F. Kessler, ESA SP-427, 23
Krause, O., Lisenfeld, U., Lemke, D., et al. 2003, A&A, 402, L1
Lagache, G., Dole, H., Puget, J.-L., et al. 2004, ApJS, 154, 112
Lemke, D., & Burgdorf, M. 1992, in Infrared Astronomy with ISO, ed. T. Encrenaz, & M. Kessler (Commack, New York: Nova Science Publishers), 69
Lemke, D., & Klaas, U. 1999, in The Universe as seen by ISO, ed. P. Cox, & M. F. Kessler, ESA SP-427, 55
Lemke, D., Klaas, U., Abolins, J., et al. 1996, A&A, 315, L64
Linden-Vørnle, M. J. D., Nørgaard-Nielsen, H. U., Jørgensen, H. E., et al. 2000, A&A, 359, 51
Mathis, J. S. 1990, ARA&A, 28, 37
Misiriotis, A., Popescu, C. C., Tuffs, R. J., & Kylafis, N. D. 2001, A&A, 372, 775
Paturel, G., Bottinelli, L., & Gouguenheim, L. 1995, Astrophys. Lett. & Comm., 31, 13
Popescu, C. C., Misiriotis, A., Kylafis, N. D., et al. 2000, A&A, 362, 138
Popescu, C. C., Tuffs, R. J., Völk, H. J., Pierini, D., & Madore, B. F. 2002, ApJ, 567, 221
Puget, J. L., Lagache, G., & Clements, D. L. 1999, A&A, 345, 29
Rowan-Robinson, M. 2001, ApJ, 549, 745
Sajina, A., Borys, C., Chapman, S., et al. 2003, MNRAS, 343, 1365
Sanders, D. B., & Mirabel, I. F. 1996, ARA&A, 34, 749
Scott, D., Lagache, G., Borys, C., et al. 2000, A&A, 357, L5
Silva, L., Granato, G. L., Bressan, A., & Danese, L. 1998, ApJ, 509, 103
Siebenmorgen, R., Krügel, E., & Chini, R. 1999, A&A, 351, 495
Sodroski, T. J., Bennett, C., Boggess, N., et al. 1994, ApJ, 428, 638
Stickel, M., Bogun, S., Lemke, D., et al. 1998a, A&A, 336, 116
Stickel, M., Lemke, D., Bogun, S., et al. 1998b, ISOPHOT far-infrared serendipity sky survey, Proc. SPIE, 3349, 115
Stickel, M., Lemke, D., Klaas, U., et al. 2000, A&A, 359, 865
Stickel, M., Lemke, D., Klaas, U., et al. 2003, in Exploiting the ISO Data Archive. Infrared Astronomy in the Internet Age, ed. C. Gry, et al., ESA SP-511, 169
Stickel, M., Lemke, D., Klaas, U., et al. 2004, A&A, 422, 39
Takeuchi, T. T., Ishii, T. T., Hirasita, H., et al. 2001, PASJ, 53, 37
Taylor, E. L., Mann, R. G., Efstathiou, A. N., et al. 2005, MNRAS, 361, 1352
Telesco, C. M. 1988, ARA&A, 26, 343
Tuffs, R. J., & Popescu, C. C. 2005, in The Spectral Energy Distribution of Gas-Rich Galaxies: Confronting Models with Data, ed. C. C. Popescu, & R. J. Tuffs, AIP Conf. Proc., 761, 344
Tuffs, R. J., Popescu, C. C., Pierini, D., et al. 2002, ApJS, 139, 37